Kurze Mitteilungen

Bis zum 15. des Monats bei der Redaktion eingehende Kurze Mitteilungen werden in der Regel am 15. des folgenden Monats veröffentlicht. Es werden auch Manuskripte aus dem Ausland angenommen, Maximalumfang: 6 Schreibmaschinenseiten (alles inbegriffen).

Energy of the So-called "Third Transition" and Intensity of Spin-forbidden Band in Chromium(III) complex of diethylamino-ethanethiol*

Summary

The electronic spectra of chromium(III) complex of diethylamino-ethanethiol have been recorded. The value of Racah's interelectronic repulsion parameter *(B)* has been evaluated and employed for the theoretical calculation of extra bands. The oscillator strength ratio of spin-forbidden to spin-allowed bands with "intensity stealing" has also been calculated.

Several recent reviews of chromium(III) spectral data[1-3] lead to the general belief that the three ligand field parameters (10 Dq, Band C) are unable to reproduce adequately the energy of the so-called "third transition" in octahedral complexes of d^3 configuration. In order to test the correctness of this statement the spectra of chromium(III) complex of diethylamino-ethanethiol-hydrochloride (DEAET) which has been characterized and described earlier[4] have been recorded in dimethyl formamide on a Hilger Uvispek spectrophotometer and the methods have been applied which may be useful to obtain a numerical fit to the relevant experimental data.

* Received February 2, 1974.

Table I. Observed and Calculated Bands in cm^{-1}
$B_{35}(Cr^{3+}$ Free ion $= 918\ cm^{-1})$

Method	$^4A_{2g} \rightarrow {}^4T_{2g}(F)$	$^4A_{2g} \rightarrow {}^4T_{1g}(F)$	$^4A_{2g} \rightarrow {}^4T_{2g}(P)$	$\delta\nu$ cm^{-1}	%	B_{35}	β_{35}
Experimental	16200	23000	34600				
a	10 Dq	Fitted	36007	1407	3.09	695	.75
b	10 Dq	21441	Fitted	−1559	7.2	496	.54
c	10 Dq	22314	35286	∓ 686	3.07 1.9	600	.65

Electronic spectra of the complex under study show four bands appearing at 13100, 16200, 23000 ($\epsilon = 15.8$), 34600 ($\epsilon = 0.6$) cm^{-1}. The band at 13100 cm^{-1} is a spin-forbidden band arising due to $^4A_{2g}(F) \rightarrow {}^2E_g$ transition. Table I records the transitions for the other three bands.

The value of 10 Dq is directly derived from the energy of the first spin-allowed band [$^4A_{2g}(F) \rightarrow {}^4T_{2g}$; 16200 cm^{-1}] and is designated as ν_1. The energies of the two higher bands are calculated from equation I:

$$\nu_{2,3} = (7.5\,B_{35} + 15\,Dq) \mp \tfrac{1}{2}[225\,B_{35}^2 + (10\,Dq)^2 - 180\,Dq \cdot B_{35}]^{1/2}. \quad I$$

The evaluation of the Racah's parameter (B_{35}) may be made by using one of the four methods[5] which differ simply by the band on which the fit is based.

(a) $B_{35} = (2\nu_1^2 + \nu_2^2 - 3\nu_1\nu_2)/(15\nu_2 - 27\nu_1)$ (Fitting the second band)

(b) $B_{35} = (2\nu_1^2 + \nu_3^2 - 3\nu_1\nu_3)/(15\nu_3 - 27\nu_1)$ (Fitting the third band)

(c) $B_{35} = (\nu_2 + \nu_3 - 3\nu_1)/15$ (Fitting the sum of second and third band)

(d) $B_{35} = 1/75\,[3\nu_1 + \{25(\nu_3 - \nu_2)^2 - 16\nu_1^2\}^{1/2}]$ (Fitting the difference of third and second band)

Equations a, b and c were applied to find out the values of B_{35} and the extra band energy was calculated from equation I. In Table I experimental transition energies are listed in line I. In the subsequent lines the calculated transition energies, their deviations from the corresponding experimental value, $\delta\nu = \nu_{calc} - \nu_{exper}$ (in cm^{-1} and in per cent) and the values of parameters B_{35} and $\beta_{35} = \frac{B_{35}\,(Complex)}{B_{35}\,(Free\ ion)}$ are given. Each line corresponds to one of the four methods applied for the evaluation of B_{35}. The values of B_{35} and β_{35} depend upon the method followed for their evaluation. The deviation ($\delta\nu$) of the calculated transition energy is very small i.e. of the order of few per cent and is largest for the method (b) and smallest for (c). If ν_2 is employed in the fit, $\delta\nu_3$ (in per cent) is smaller than $\delta\nu_2$ which follows if ν_3 is used. Finally in method (c), $|\delta\nu_2| = |\delta\nu_3|$.

Therefore it is evident that within the approximation of three parameters of ligand field theory, the energies of both second and third bands are reproduced equally well. In addition to this there simply does not exist a misfit of ν_3 which could be redistributed on ν_2 and ν_3 if method (c) is employed. If this were correct, one expects a value of $\delta\nu$ intermediate between $\delta\nu$(a) and $\delta\nu$(b). However $\delta\nu$(c) is always smaller than $\delta\nu$(a) and $\delta\nu$(b).

If the spin-forbidden band "steals" intensity from the first spin-allowed band, then the ratio of oscillation strengths is given by[6]

$$\frac{f_{SF}}{f_{SA}} = \frac{4}{9} \cdot \frac{\omega_{SF}}{\omega_{SA}} \cdot \frac{\xi^2}{(\omega_{SA} - \omega_{SF})^2},$$

where ω_{SF} and ω_{SA} are the wave numbers of the maxima of spin-forbidden and spin-allowed bands respectively and ξ is the spin-orbit coupling parameter (for a d^3 ion $\xi = 3\lambda$). The value of λ (spin-orbit coupling constant) has been evaluated from the following equation –

$$g = 2 - 8\lambda/10\,Dq,$$

where g is Lande's splitting factor, the value of which is 1.953 (from E.P.R. studies[4] of the complex under study).

The ratio f_{SF}/f_{SA} comes out to be 304.4×10^{-5} which is of the order of oscillator strength ratio of spin-forbidden (Laporte-forbidden) to spin-allowed (Laporte-forbidden but with "intensity stealing")[7].

P.C. Jain

School of Chemistry, Meerut College, Meerut (India)

[1] L.S. Forster, *Transition Metal Chem. 5* (1969) 1.
[2] D. Reinen, *Struct. Bonding* (Berlin) *6* (1969) 30.
[3] C. K. Jørgensen, *Oxidation numbers and oxidation states*, Verlag Springer, Berlin 1969.
[4] P.C. Jain and H.L. Nigam, *Indian J. Chem. 8* (1970) 456–7.
[5] J.R. Perumareddi, *Naturforsch. 22* (1967) 908.
[6] Y. Tanabe, *Suppl. Progr. Theor. Phys.* (Osaka) *14* (1960) 17.
[7] B.N. Figgis, *Introduction to Ligand Fields*, Interscience Publishers Inc., New York 1967, p. 209.

Formation of Print-Out Images on Large Crystals of Lead Chloride*

Summary

The presence of oxygen during exposure influences the formation of print-out images obtained on large crystals of lead chloride. The photolysis of these crystals can be divided into three different steps as a function of the exposure time:

1) Short exposure times corresponding to the latent image,
2) longer exposures lead to a print-out image if they are made in the absence of oxygen, and to an invisible one in the presence of oxygen,
3) very long exposures give a print-out image (in the presence as well as in the absence of oxygen).

For the same crystal and equally long exposure times, the visible image obtained in the presence of oxygen penetrates deeper into the crystal bulk than in the absence of oxygen. If an exposure in air follows an exposure in the absence of oxygen, a bleaching of the print-out occurs. These phenomena are interpreted as resulting from the photo-oxidation of lead nuclei by the oxygen molecules adsorbed at the crystal surface. As shown by diffuse reflectance measurements, the reflectance of exposed crystal surfaces of $PbCl_2$ varies with the square root of the exposure time up to certain saturation limit.

Introduction

In previous works[1-4] concerning the formation of latent images on large crystals of lead halides, we have shown that it is possible to develop latent images by two different techniques. These methods allow us to develop two types of latent images having different properties. The photochemical behaviour of lead halides is strongly depending on the presence of oxygen during exposure to light [1-4].

The image obtained in the absence of oxygen is formed by lead nuclei and can be developed by means of a physical developer[2] acting by the selective reduction of silver ions on lead nuclei. The image obtained in the presence of oxygen is not possible to be developed by this technique, but it can be developed by etching with a solvent. We have assumed that in this latter case, the latent image was formed by lead oxyhalides resulting from the photo-oxidation of the lead halide by the oxygen molecules adsorbed at the crystal surface. We have shown that this photo-oxidation depends on the pressure of oxygen, the light intensity, the exposure time and the photosensitivity of the $PbCl_2$ crystal.

Based on these results, we have proposed a mechanism for the photolysis of lead halides in which the reducing action of the photoelectrons at the crystal surface plays an important role.

The formation of the print-out image in lead halides has already been studied by several authors[5-10], but only little attention was given to the influence of oxygen during exposure. Particularly, Kaldor and Somorjai[6] have observed that no image is produced on $PbCl_2$ exposed in air. Verwey[9] noticed that the subsequent illumination of a $PbCl_2$ crystal at 365 nm in presence of oxygen and previously exposed under vacuum produced a bleaching of the print-out image.

* Received May 5, 1974.

In this work, we describe some new observations concerning the influence of oxygen on the print-out image. The photochemical decomposition of large crystals of $PbCl_2$ is also followed by diffuse reflectance measurements.

Experimental

The preparation of $PbCl_2$ crystals from the melt by the method of Bridgman-Stockbarger[11], their polishing and their characterization is described elsewhere[1,4]. Chemically polished crystals of $PbCl_2$ were then exposed at room temperature to a polychromatic beam of light coming from a mercury lamp. The intensity absorbed by the $PbCl_2$ is in the order of 10^{14} to 10^{15} quanta $\cdot s^{-1} \cdot cm^{-2}$. Exposures were made either in air or under vacuum (10^{-5} torr)[1]. The exposure time varied between 15 min and 24 h.

Diffuse reflectance measurements were made with a spectrophotometer «Zeiss» (model PMQ II with double monochromator MM 12 and with reflectance device KA). $PbCl_2$ crystals, mechanically polished to increase their reflecting power, were placed on an aperture (4×5 mm) made in an Ulbricht sphere interiorly covered with magnesium oxyde. The intensity of the light reflected by the crystal surface was measured with a photomultiplier. A plate of magnesium oxyde was used as a reference. Crystals are illuminated in air directly in the reflectance device (without objective).

Results

Influence of oxygen on the print-out image

Table I gives a qualitative description of our results obtained from the photolysis of large crystals of $PbCl_2$.

Table I. Description of print-out images obtained on $PbCl_2$

	Exposure time	Print-out image	Observations
Under vacuum	0 to 2 h	None	
Under vacuum	2 to 24 h	Black image	Superficial, not homogeneous, fading of developable image
In air	0 to 6 h	None	
In air	6 to 24 h	Brown image	Homogeneous, internal, stable developable image
Under vacuum, then in air	> 2 h (vacuum) 0 to 6 h (air)	Clearer band in the zone exposed in air (fig. 1)	Cannot be physically developed
Under vacuum, then in air	> 2 h (vacuum) > 6 h (air)	Bronw band in air	Internal, physically developable
In air, then under vacuum	< 6 h (air) > 2 h (vacuum)	Darker band in the zone exposed in air	Physically developable image

Study of the photolysis by diffuse reflectance measurements

Fig. 2 shows reflectance spectra obtained on four different non illuminated crystals of lead chloride. These measurements were influenced by the surface roughness of the crystals.

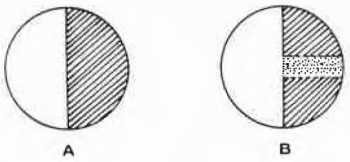

Fig. 1. Scheme of a $PbCl_2$ crystal showing the bleaching effect: A. Image obtained after an exposure under vacuum (shaded area). B. Image formed after the second exposure in air (clearer band in shaded area)

The general form of our reflectance spectra is similar to that of the absorption spectrum of $PbCl_2$. The reflectance peak at 272 nm corresponds to the absorption band observed by Kojima and Yanada[12] (270 nm), Hilsch and Pohl[13] (271 nm), De Vries and Van Santen[14] (270 nm), and Canit[15] (274 nm). This absorption band is probably due to the formation of an exciton which requires approximately 0,7 eV less energy than the excitation of an electron into the conduction band[16, 17]. The two secondary maxima situated at 307 nm and between 318 and 321 nm were not visible in the absorption spectra. They may be explained by the fact that above the absorption edge some inactinic light is reflected from the other face of the crystal. It is also possible that these maxima are due to a slight hydrolysis of the surface by humidity, giving absorption bands similar to those described by Kojima and Yanada[12].

Fig. 3 shows the evolution of the reflectance spectrum of a large crystal of $PbCl_2$ exposed to UV light.

On all the samples, the illumination produced a distinct decrease of reflectance between 300 and 400 nm, and a weaker one above 400 nm. For this sample (fig. 3), the reflectance was not changed under 290 nm upon illumination. However, other samples showed a small reflectance decrease also at $\lambda < 260$ nm. At long exposures ($\geq$ 5 h), the reflectance spectrum gets a similar form as the absorption spectrum and does not change subsequently.

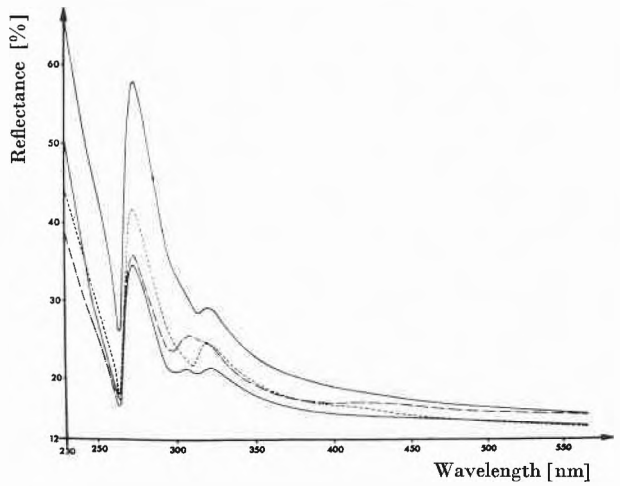

Fig. 2. Diffuse reflectance spectra of four different $PbCl_2$ crystals. The differences between the curves are principally due to differences of the surface roughness

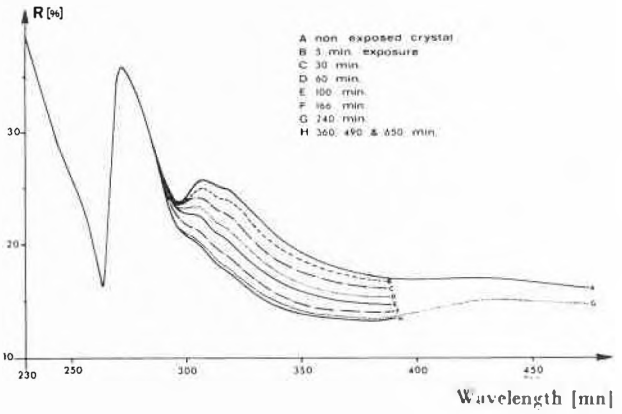

Fig. 3. Influence of the exposure on the reflectance spectrum of a $PbCl_2$ crystal (exposure in air)

In order to compare different samples, we have calculated the ratio R/R_0, where R_0 is the reflectance of the unexposed crystal (taken arbitrarily at 330 nm).

Fig. 4, on which we have plotted R/R_0 *versus* the square root of the exposure time ($min^{1/2}$), shows the results obtained for three different crystals.

The curves slopes of which are respectively $-0{,}018$, $-0{,}020$, and $-0{,}029$ $min^{1/2}$, show that the reflectance decreases approximately linearly as a function of the square root of the exposure time, except in the first part of the upper curve, where it is a linear function of the exposure time. This result is similar to those obtained by Morantz et al.[10] (on pressed pellets of $PbBr_2$), Dawood et al.[18, 19] (thin layers of PbI_2) and Verwey[8] (monocrystals of $PbCl_2$, $PbBr_2$ and PbI_2). In the case of $PbCl_2$, this author also observed a linear relation between the photolysis and the exposure time in the first part of the curve.

Discussion

From our results on the influence of oxygen on the print-out image and from those obtained in the range of the latent image[1–4], we propose the following scheme for the evolution of the photolysis of large crystals of lead chloride.

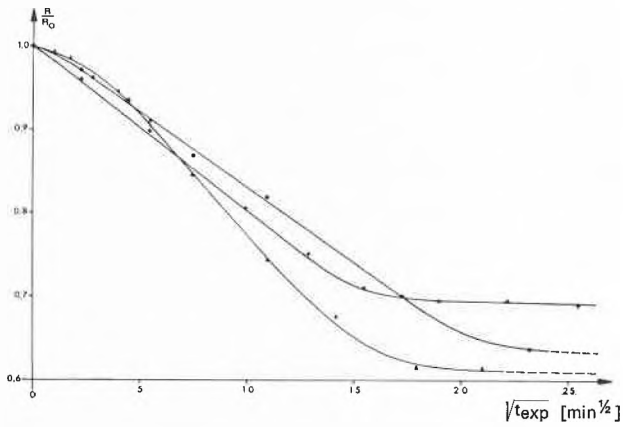

Fig. 4. R/R_0 at 330 nm *versus* the square root of the exposure time

The photolysis of polished crystals of $PbCl_2$ shows three distinct steps, each depending on the quality of the crystal, the oxygen pressure during exposure, and the light intensity.

1) During the *first step*, no print-out image is observed. This is the range of the so called "latent image".
   - In presence of oxygen, lead oxychloride ($x PbO \cdot y PbCl_2$) is formed by trapping of the photoelectrons by oxygen molecules adsorbed at the crystal surface. In this case, an image can only be developed by etching[1].
   - In absence of oxygen, the latent image is formed with lead particles, developable by means of a physical developer[2,3].
2) In the *second step*, the exposure in absence of oxygen* gives a visible image. This image, developable by etching, can also be developed by physical development. The presence of lead nuclei is probably due to the photodecomposition of surface aggregates of lead oxide according to the reaction[3,4]

   $PbO \xrightarrow{h\nu} Pb + 1/2\ O_2$.
3) During the *third step*, a print-out image is observed, whether exposures are made in presence or in absence of oxygen.

In the case of exposures in air, the brown surface image is probably composed of lead oxide and metallic lead. The internal part of this image is black and has the same width as the beam of light. Our observations that light contributes to the effect of penetration of the image, although the largest part of the absorbed light does not penetrate deeper than approximately 0,3 μ[9,20], may suggest that photons which are not absorbed by lead chloride participate to the effect of penetration of the image. As the presence of oxygen is necessary during exposure to obtain an internal image, oxygen must produce a surface modification such that the photolytic properties of the crystal are changed.

The bleaching of the print-out image if the exposure in air follows the exposure under vacuum corresponds to the disappearance of the image also observed in the range of the latent image[3] under the same exposure conditions. The regression of the print-out image is attributed to the photo-oxidation of a part of the lead particles by the oxygen molecules adsorbed at the crystal surface. This regression may be explained by two complementary mechanisms:

1) The absorption of photons by lead nuclei produces the excitation of conduction electrons of lead into the conduction band of the crystal. These electrons move towards the crystal surface where they are trapped by adsorbed oxygen molecules. This mechanism is supported by the effect of secondary photo-oxidation described in [3].
2) The photogenerated holes produced in the crystal can be trapped by the lead nuclei while the photoelectrons can react with the oxygen molecules adsorbed at the crystal surface to form O^{-2} ions.

The observed bleaching of the print-out image results from a decrease of the concentration of lead nuclei associated with the surface oxidation.

The variation of the photolysis with the square root of the exposure time could be due, according to Morantz et al.[10] and to Dawood et al.[18,19], to the diffusion of positive holes through a surface layer enriched in lead particles. Fig. 4 shows that the decrease of the reflectance stops after a certain exposure time. As already observed by Morantz et al.[10], the saturation effect obtained for long exposure times is very pronounced in the case of our crystals where photolysis seems to stop completely. That observation may be related to the penetration of the image in the crystal. The stopping of the photolysis observed by diffuse reflectance may only be apparent. It is eventually due to an equilibrium between the formation of surface lead nuclei and their oxidation by the holes coming from the bulk. The presence of an internal image if exposures are made in air suggests that lead nuclei can form in deeper layers of $PbCl_2$ crystals, without changing the reflecting power of the surface.

Acknowledgement

The authors wish to thank Dr. P. Junod of CIBA-GEIGY Photochemie Ltd. for helpful discussions.

Bibliography

1 J.-F. Reber, J. G. Fernandez-Garcia, R. Steiger und Ch. G. Boissonnas, *Helv. Chim. Acta 55* (1972) 1436.
2 J.-F. Reber et al., *Chimia 27* (1973) 27.
3 J.-F. Reber et al., to be published in *Photogr. Sci. Eng. 1974.*
4 J.-F. Reber, Thesis, University of Neuchâtel, 1973.
5 C. Renz, *Z. anorg. Chem. 116* (1921) 62.
6 A. Kaldor and G. A. Somorjai, *J. Physic. Chem. 70* (1966) 3538.
7 J. F. Verwey, *J. Physic. Chem. Solids 27* (1966) 468.
8 J. F. Verwey, ibid. *3* (1970) 163.
9 J. F. Verwey, Thesis, Utrecht 1967.
10 D. J. Morantz, R. A. M. Scott and J. J. Shortland, *J. Physic. Chem. Solids 33* (1972) 1235.
11 H. E. Buckley, *Crystal Growth*, Wiley, New York 1951, p. 77.
12 M. Kojima and T. Yanada, *Sci. Rep. Tohoku Univ. I. Ser. 45* (1961) 23.
13 R. Hilsch and R. W. Pohl, *Z. Physik 48* (1928) 384.
14 K. J. De Vries and J. H. Van Santen, *Physica 30* (1964) 2051.
15 J. C. Canit, *Physic. Status Solidi 38* (1970) K 153.
16 K. J. Best, *Z. Physik 163* (1961) 309.
17 N. L. Kramarenko, V. K. Miloslavskii and Y. V. Naboikin, *Ukr. Fiz. Zh. 15* (1970) 416.
18 R. I. Dawood and A. J. Forty, *Phil. Mag. 7* (1962) 1633.
19 R. I. Dawood, A. J. Forty and M. R. Tubbs, *Proc. Roy. Soc. 284* (1965) 272.
20 W. C. De Gruijter and J. Kerssen, *Solid State Commun. 10* (1972) 837.

Jean-François Reber*, José G. Fernandez-Garcia, Rolf Steiger*, and Charles G. Boissonnas

Institut de chimie de l'Université, 2000 Neuchâtel, Switzerland

* No print-out image is observed if the exposure is made in presence of oxygen.

* Present address: CIBA-GEIGY Photochemie Ltd., 1701 Fribourg, Switzerland. Requests may be addressed to J.-F. Reber.

Band Assignments in the Infrared Spectra of p-Toluidine and Its Complexes with Metal(II) Chlorides*

Summary

The infrared spectra of *p*-toluidine and its complexes with $CoCl_2$, $NiCl_2$, $CuCl_2$ and $ZnCl_2$ are discussed. ^{15}N-Labelling of the nitrogen atom is used to assign bands originating in the vibrations of the amino-group. The metal-nirogen stretching frequencies ($\nu M—N$) are assigned to bands which are sensitive to ^{15}N-labelling and which shift on varying the coordinated metal ion in the expected sequence of metal–ligand bond stabilities: Co > Ni < Cu > Zn.

The infrared spectra of metal complexes of aromatic amines have received considerably less attention than those of heterocyclic amines[1]. The spectra of several complexes with the general formula $[ML_2X_2]$ (L = aromatic amine, X = halogen) have been reported[2–4] but no definite conclusions on the assignment of $\nu M—N$ were reached. We now report the application of two techniques (^{15}N-labelling and metal ion substitution) to the assignment problem in the complexes [M(*p*-toluidine)$_2$Cl$_2$] (M = Co, Ni, Cu, Zn).

Bands exhibiting significant ^{15}N-induced shifts in the infrared spectrum of *p*-toluidine are listed in Table I. Dilute (0.05 molar) solutions in carbon tetrachloride were used in order to avoid hydrogen bonding effects. The frequencies, isotopic shifts and assignments correspond very closely with those reported by TSUBOI[5] for aniline. The NH_2 wagging frequency has not been assigned with certainty in the spectrum of aniline. In primary aliphatic amines, this vibration is reported[6] to yield a broad band within the range 750 to 850 cm^{-1}. The only ^{15}N-sensitive band within this region in the spectrum of *p*-toluidine occurs at 811.8 cm^{-1} and is therefore tentatively assigned to the NH_2 wagging mode.

Spectroscopic data for the complexes are given in Table II and their far infrared spectra are depicted in Fig. 1. The bands between 3200 and 3400 cm^{-1} correspond with the $\nu N—H$ bands of the ligand shifted some 150 to 200 cm^{-1} towards lower frequency by coordination. The bands near 3100 cm^{-1} almost certainly originate in the N—H ... Cl species[7]. ^{15}N-Sensitive bands are observed some 20 to 70 cm^{-1} below the bands assigned to the NH_2 deformation vibrations and $\nu C—N$ in the ligand spectrum. The region of $\nu C—N$ absorption corresponds with that previously reported in empirical[4] and ^{15}N-labelling[8] studies of complexes containing coordinated primary aromatic amines. A band near 740 cm^{-1} occurs in the spectrum of each complex. Its position and ^{15}N-sensitivity support its assignment to the NH_2 wagging mode.

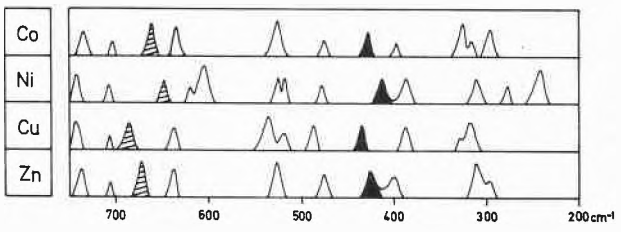

Fig. 1. Infrared spectra of [M(*p*-toluidine)$_2$Cl$_2$]. The NH_2 rocking bands are shaded and the $\nu M—N$ bands are solid

Table I. Comgarison of vibrational frequences, ^{15}N-induced shifts ($\Delta\nu$) and assignments from the infrared spectra of *p*-toluidine and aniline in dilute carbon tetrachloride

p-Toluidine Frequency (^{14}N) (cm^{-1})	$\Delta\nu$ (cm^{-1})	Aniline[5] Frequency (^{14}N) (cm^{-1})	$\Delta\nu$ (cm^{-1})	Assignment
3486.0	− 8.2	3481.4	− 9.7	$\nu N—H$ antisym.
3398.7	− 4.4	3395.2	− 5.4	$\nu N—H$ sym.
1628.0	− 2.2	1618.9	− 6.0	NH_2 scissors
1274.7	− 4.0	1276.1	− 5.2	$\nu C—N$
1126.4	− 0.9	1114.6	− 2.4	NH_2 twist
811.8*	− 0.7			NH_2 wag

* In 0.05 molar cyclohexane

Crystallographic studies[9,10] and electronic spectra[3] have firmly established that the Ni(II) complex has polymeric octahedral coordination (with bridging chlorine atoms) while the Co(II) and Zn(II) complexes are tetrahedral and the Cu(II) complex is either square planer or tetragonal with weak axial Cu—Cl bonds. In a series of complexes of these structures, the Irving-Williams[11] stability sequence: Co < Ni < Cu > Zn becomes deranged[12] to Co > Ni < Cu > Zn. The difference arises from the fact that the IRVING-WILLIAMS sequence is based on octahedral Co(II) and Ni(II) and tetragonal (or square planar) Cu(II) whereas in the *p*-toluidine complexes, the presence of 4-coordinate Co(II) implies that each cobalt-ligand bond acquires greater stability than it would achieve in 6-coordinate octahedral coordination. It is now well-established[12–14] that metal-ligand stretching frequencies follow the order of metal-ligand bond stabilities in a series of complexes containing metal ions of the first transition series. In order to assign $\nu M—N$ in the *p*-toluidine complexes, we therefore seek bands which satisfy two criteria: significant ^{15}N-sensitivity and a metal ion dependence in the order Co > Ni < Cu > Zn. The two bands which best satisfy these criteria occur within the ranges 640 to 700 and 400 to 450 cm^{-1}. Of these two bands, it would be unreasonable to assign that within the range 640 to 700 cm^{-1} to uncoupled $\nu M—N$ since all available data[1] indicates that $\nu M—N$ in metal complexes does not exceed 600 cm^{-1}. More likely, this band originates in the NH_2 rocking mode which is generally observed within the range 600 to 700 cm^{-1}. It is well known[13,15] that,

* Received May 6, 1974.

Table II. Assigned bands in the infrared spectra of the complexes $[M(p\text{-toluidine})_2Cl_2]$ (^{15}N-induced shifts in parenteses)

M→	Co (cm^{-1})	Ni (cm^{-1})	Cu (cm^{-1})	Zn (cm^{-1})	Assignment
3280	(− 19)	3322 (− 8)	3300 (− 7)	3274 (− 7)	νN—H antisym.
		3313 (− 7)			
3236	(− 13)	3253 (− 6)	3234 (− 5)	3231 (− 4)	νN—H sym.
		3236 (− 5)			
3136	(− 11)	3130*	3118 (− 13)	3136 (− 6)	νN—H ... Cl
1582	(− 5.7)	1587 (− 3.6)	1567 (− 2.0)	1583 (− 5.1)	NH_2 scissor
		1571 (− 4.6)			
1242*		1253 (− 4.9)	1240*	1242 (− 6.7)	
1223	(− 2.6)	1239 (− 2.7)	1221	1224 (− 3.8)	νC—N
		1225			
1214		1209 (− 3.7)		1215 (− 2.6)	
		1163 (− 1.5)	1149 (− 3.2)	1149 (− 3.3)	
1097	(− 10.5)	1062 (− 5.2)	1093 (− 9.0)	1101 (− 9.4)	NH_2 twist
		1030 (− 2.1)			
737	(− 6.5)	743 (− 6.1)	743 (− 9.5)	739 (− 6.0)	NH_2 wag
			706 (− 3.5)		
663	(− 2.4)	649 (− 1.5)	685 (− 5.8)	674 (− 7.0)	NH_2 rock
636		620 (− 3.6)	639	638	
		608 (− 4.4)			
525	(− 1.7)	525 (− 1.9)	535 (− 4.1)	528 (− 2.2)	coupled νM—N (?)
		519 (− 1.7)	518 (− 3.6)		
475	(− 4.0)	479 (− 4.0)	488	475 (− 5.0)	coupled νM—N (?)
426	(− 1.7)	414 (− 3.6)	445 (− 7.7)	423 (− 4.4)	νM—N
400	(− 2.9)	387	388	399 (− 2.0)	
326			327 (− 3.5)		
316	(− 1.6)	311 (− 2.0)	308 (− 1.8)	311	
296		276 (− 1.5)		299	

* Weak and broad band; frequency and shift cannot be determined precisely

among the vibrations of the amino group, the NH_2 rocking frequency exhibits a particularly marked shift on varying the coordinated ion.

The band within the range 400 to 450 cm^{-1} remains for assignment as the principal (least-coupled) νM—N band on the basis of its substantial ^{15}N-sensitivity and its significant metal ion dependence in the order Co > Ni < Cu > Zn. Its position is, moreover, consistent with previous assignments[13, 16] of νM—N in the complexes $[M(hydrazine)_2Cl_2]$ and $[M(NH_3)_2Cl_2]$ (M = Co, Ni, Cu, Zn).

The present work implies that certain assignments, previously made on a purely empirical basis, require revision. In particular, some bands previously assigned[3] as "most likely derived from M—N vibrations" exhibit no ^{15}N-sensitivity while other bands, previously assigned[3] to νM—Cl, are now found to shift appreciably on ^{15}N-labelling. If the νM—Cl assignments are correct, appreciable coupling from a vibration involving the nitrogen atom must occur.

Experimental

The ^{14}N-complex were precipitated from ethanol solution containing the stoichiometric quantities of the metal chloride and *p*-toluidine. Purity was established by microanalysis. The ^{15}N-complexes were similarly prepared from ^{15}N-*p*-toluidine (95 atom per cent isotopic purity) supplied by Prochem Ltd. Infrared spectra were determined on Nujol mulls between caesium iodide plates on a Beckman IR-12 spectrophotometer. At least five determinations of each ^{15}N-sensitive band were made. The spectra of ^{14}N- and ^{15}N-*p*-toluidine were determined on 0.05 molar solutions in carbon tetrachloride and cyclohexane,

Acknowledgements

We thank the Univerity of Cape Town Research Grants Committee for financial assistance.

P. R. Johnson

Department of Inorganic Chemistry
University of Cape Town (South Africa)

D. A. Thornton

Department of Physiology and Medical Biochemistry
University of Cape Town (South Africa)

[1] D. M. Adams, *Metal-Ligand and Related Vibrations*, Edward Arnold, London 1967, p. 268.
[2] I. S. Ahuja, D. H. Brown, R. H. Nuttall and D. W. A. Sharp, *J. Inorg. Nucl. Chem. 27* (1965) 1105.
[3] I. S. Ahuja, D. H. Brown, R. H. Nuttall and D. W. A. Sharp, *J. Inorg. Nucl. Chem. 27* (1965) 1625.
[4] M. A. J. Jungbauer and C. Curran, *Spectrochim. Acta 21* (1965) 641.
[5] M. Tsuboi, *Spectrochim. Acta 16* (1960) 505.
[6] J. E. Stewart, *J. Chem. Physics 30* (1959) 1259.
[7] J. Chatt, L. A. Duncanson and L. M. Venanzi, *J. Chem. Soc. 1956*, 2712.
[8] C. A. Fleming and D. A. Thornton, *Spectroscopy Letters 6* (1973) 245.
[9] G. B. Bokii, T. I. Malinovskii and A. V. Ablov, *Kristallografiya 1* (1956) 49.
[10] A. V. Ablov and T. I. Malinovskii, *Dokl. Akad. Nauk SSSR 123* (1958) 677.
[11] H. Irving and R. J. P. Williams, *J. Chem. Soc. 1953*, 3192.
[12] J. M. Haigh, R. D. Hancock, L. G. Hulett and D. A. Thornton, *J. Mol. Structure 4* (1969) 369.
[13] L. Sacconi and A. Sabatini, *J. Inorg. Nucl. Chem. 25* (1963) 1389.
[14] L. G. Hulett and D. A. Thornton, *Spectrochim. Acta 27A* (1971) 2089.
[15] G. F. Svatos, D. M. Sweeny, S. Mizushima, C. Curran and J. V. Quagliano, *J. Amer. Chem. Soc. 79* (1957) 3313.
[16] R. J. H. Clark and C. S. Williams, *J. Chem. Soc.* (A) *1966*, 1425.

Pouvoir discriminatoire du palladium (II) dans les réactions de substitution de ses chlorocomplexes avec les diamines*

Summary

The rate constants of the substitution reactions of chloride and water by various diamines in chlorocomplexes of Pd(II) have been determined spectrophotometrically. The mechanism of substitution is associative and the comparison with the corresponding Pt(II) complexes shows that the discriminating power of Pd(II) is smaller than the one of Pt(II).

Dans une communication précédente[1], nous avons reporté l'étude cinétique de la réaction de substitution en solution aqueuse:

$$PdCl_4^{2-} \xrightarrow{am} Pd(am)Cl_2 \xrightarrow{am} Pd(am)_2^{2+}$$

avec am = éthylènediamine (en).

Nous avons étendu cette étude à d'autres diamines aliphatiques: la 1,2-diméthyléthylènediamine (Me_2en), l'homopipérazine (hp) et la tétraméthyléthylènediamine (Me_4en). Le schéma réactionnel des deux étapes de la substitution sur ces complexes carrés d^8 est:

$$PdCl_4^{2-} + H_2O \underset{k_{-1}\,(\text{rapide})}{\overset{k_1}{\rightleftharpoons}} Pd(H_2O)Cl_3^- + Cl^-$$

$$Pd(H_2O)Cl_3^- + amH^+ \xrightarrow{k_{s1}} Pd(am)Cl_2 + Cl^- + H^+ + H_2O$$

$$PdCl_4^{2-} + amH^+ \xrightarrow{k_{c1}} Pd(am)Cl_2 + 2Cl^- + H^+$$

$$Pd(am)Cl_2 + H_2O \underset{\text{rapide}}{\overset{K_2}{\rightleftharpoons}} Pd(am)(H_2O)Cl^+ + Cl^-$$

$$Pd(am)(H_2O)Cl^+ + amH^+ \xrightarrow{k_{s2}} Pd(am)_2^{2+} + Cl^- + H^+ + H_2O$$

$$Pd(am)Cl_2 + amH^+ \xrightarrow{k_{c2}} Pd(am)^{2+} + 2Cl^- + H^+$$

Toutes les réactions étudiées sont du premier ordre en substrat et en nucléophile. Les substrats sont le chlorocomplexe et son monoaquocomplexe et la forme réagissante de la diamine est amH^+[1]. La détermination de la stœchiométrie de la réaction, de l'identité des espèces et des constantes de vitesse observées a été obtenue par spectrophotométrie[1]. Dans le cas général d'une réaction de substitution par Y dans un complexe L_3MX, en équilibre avec son aquocomplexe $L_3M(H_2O)$, la loi cinétique théorique est:

$$d[L_3MY]/dt = k_{ob}[L_3MX] = \left[\frac{k_1[H_2O][Y]/[X]}{k_{-1}/k_s + [Y]/[X]} + k_c[Y]\right][L_3MX]. \quad (1)$$

Dans notre cas et pour les deux étapes, nous avons étudié la variation de k_{ob} en fonction de [am] et de [Cl^-] et obtenu la loi cinétique expérimentale: $k_{ob} = Kk_s[Y]/[X] + k_c[Y]$ avec $Y = amH^+$, $X = Cl^-$ et $K = [H_2O]k_1/k_{-1}$. Comme dans nos conditions expérimentales[1], nous avons toujours l'inégalité $k_{-1}/k_s \ll [Y]/[X]$, la loi cinétique (1) est vérifiée. Les constantes de vitesse individuelles sont reportées dans le Tableau 1.

Tableau 1. Constantes de vitesse de substitution par quelques diamines [25 °C; $\mu = 1{,}0$ ($NaClO_4$)]

Réaction	k_c ($M^{-1}s^{-1}$)	k_sK^* (s^{-1})	$10^{-2}k_s$ ($M^{-1}s^{-1}$)
$PdCl_4^{2-} + NH_3$ [3]	33	30	7,1
$PdCl_4^{2-} + enH^+$	296 ± 44	146 ± 24	35
$PdCl_4^{2-} + Me_2enH^+$	153 ± 25	67 ± 12	16
$PdCl_4^{2-} + hpH^+$	133 ± 19	84 ± 4	20
$PdCl_4^{2-} + Me_4enH^+$	14 ± 1	5,1 ± 0,3	1,2
$Pd(en)Cl_2 + 2NH_3$	42 ± 6	13 ± 1	0,9
$Pd(en)Cl_2 + enH^+$	81 ± 4	19 ± 2	1,3
$Pd(en)Cl_2 + Me_2enH^+$	20 ± 3	1,5 ± 0,5	0,1
$Pd(en)Cl_2 + hpH^+$	15 ± 5	4,6 ± 0,5	0,3
$Pd(en)Cl_2 + Me_4enH^+$	1,6 ± 0,2	–	
$Pd(Me_2en)Cl_2 + Me_2enH^+$	9 ± 1	1,6 ± 0,1	
$Pd(hp)Cl_2 + hpH^+$	18 ± 7	12 ± 1	

* $K_1 = [Pd(H_2O)Cl_3^-][Cl^-]/[PdCl_4^{2-}] = 0{,}042$.[2]
$K_2 = [Pd(en)(H_2O)Cl^+][Cl^-]/[Pd(en)Cl_2] = 0{,}015 \pm 0{,}002$.[4]

Réactivité des différentes amines

Rund[5] a constaté que la vitesse de substitution du chlorure dans $PdCl_4^{2-}$ par différentes *o*-phénanthrolines est indépendante de la basicité de celles-ci. Par contre, Cattalini[6] trouve une relation linéaire entre la constante de vitesse de 2e ordre ($\lg k_2$) et le pK_a de différentes pyridines dans le cas du substrat $Pd(PhSCH_2CH_2SPh)Cl_2$ (groupe de départ: Cl^-). Dans notre cas, nous n'avons pas trouvé de relation entre les constantes de vitesse k_c et k_s et la basicité des différentes diamines examinées. La comparaison des constantes k_c et k_s pour les différentes diamines donne dans chaque cas la séquence (en > hp, $Me_2en \gg Me_4en$); la réactivité d'une diamine diminue si le nombre de groupes alkyles fixés sur l'azote augmente. La réaction $Pd(Me_4en)Cl_2 + Me_4en$ n'a pas lieu à *p*H 4–5, même en présence d'un fort excès de Me_4enH^+. Ceci est certainement dû à l'effet stérique des groupes méthyles qui empêche la fixation ultérieure d'une amine tertiaire. En milieu alcalin, on observe la formation d'un mélange de $Pd(Me_4en)(OH)Cl$ et $Pd(Me_4en)(OH)_2$.

* Reçu le 4 juin 1974.

Tableau 2. Effet du groupe de départ et effet du groupe *trans*

	$\frac{PdCl_4^{2-}}{Pd(en)Cl_2}$	$\frac{Pd(H_2O)Cl_3^-}{Pd(en)(H_2O)Cl^+}$	$\frac{Pd(H_2O)Cl_3^-}{PdCl_4^{2-}}$	$\frac{Pd(en)(H_2O)Cl^+}{Pd(en)Cl_2}$
	k_{cl}/k_c *	k_{sl}/k_s	k_{sl}/k_{cl}	k_s/k_c
NH_3 **	> 0,8	8	< 22	21 ± 3
enH^+	4 ± 1	27 ± 5	12 ± 3	16 ± 2
Me_2enH^+	7 ± 2	160 ± 76	11 ± 3	5 ± 2
hpH^+	9 ± 3	67 ± 8	15 ± 2	21 ± 7
Me_4enH^+	9 ± 1	très grand	9 ± 1	> 5

* k_c et k_s sont les constantes de vitesse de substitution des différentes diamines sur $Pd(en)Cl_2$ et $Pd(en)(H_2O)Cl^+$, respectivement.
** Pour NH_3, les valeurs de k_{cl} et k_{sl} sont celles de Reinhardt[3].

Réactivité des différentes substrats

Les rapports des colonnes 1 et 2 sont supérieurs à un, donc l'effet *trans* de Cl^- est plus grand que celui d'une amine, comme c'est le cas pour Pt(II). Les rapports des colonnes 3 et 4 sont également supérieurs à un, donc H_2O est un meilleur groupe de départ que Cl^-. Les rapports k_s/k_c sont analogues à k_{sl}/k_{cl}. Si le substrat $Pd(en)ClX$ ($X = Cl^-$, H_2O) est moins sensible à la nature du groupe de départ X que $PdCl_3X$, cela signifie que, par rapport à $Pd(en)ClX$, la scission de la liaison Pd—X du substrat $PdCl_3X$ est plus importante que la formation de la liaison Pd-am en tant que facteur déterminant la vitesse de réaction. Donc $Pd(en)ClX$ doit être plus sensible à la nature du groupe entrant que $PdCl_3X$. C'est bien ce que l'on observe car la variation de k_s/k_c est plus importante que celle de k_{sl}/k_{cl} en fonction des différentes diamines entrantes. De même, le rapport k_{sl}/k_s varie plus fortement que k_{cl}/k_c, donc la formation de la liaison Pd-am est relativement plus importante que la scission de Pd—X dans le cas des aquocomplexes que dans celui des chlorocomplexes. L'encombrement stérique dû aux groupes alkyles de l'amine n'est marqué que dans le cas de la réaction $Pd(Me_4en)Cl_2 + Me_4en$ où la substitution de Cl^- n'a pas lieu.

Comparaison entre Pd(II) et Pt(II) comme atome central

En comparant nos résultats à ceux de Kukushkin[7], on obtient $k_{cl}(Pd)/k_{cl}(Pt) = 1{,}5 \cdot 10^5$ pour en et $2{,}5 \cdot 10^5$ pour Me_4en. Les complexes de Pd(II) réagissent environ 10^5 fois plus rapidement que ceux de Pt(II) et l'ordre de grandeur est le même que dans le cas des réactions $M(dien)X^+ + py$ ($X = SCN^-$, NO_2^-)[8].

Il reste à comparer le pouvoir discriminatoire de Pd(II) envers les nucléophiles à celui de Pt(II). Ce dernier peut être exprimé par la différence $|\lg k_1 - \lg k_c|$ pour MCl_4^{2-} et par $|\lg k_s - \lg k_{-1}|$ pour $M(H_2O)Cl_3^-$. Les constantes k_1 et k_{-1} ont été mesurées par Elding (Pd[9], Pt[10]). Les valeurs de k_s pour $Pt(H_2O)Cl_3^-$ sont inconnues. Cependant, comme la loi cinétique générale du Pt(II) est[11]: $k_{ob} = k_1[H_2O] + k_c[Y]$, la constante de vitesse de l'étape déterminante de la substitution via l'aquocomplexe est k_1; on a $k_s \gg k_1$ et donc $|\lg k_s - \lg k_{-1}| > |\lg k_1 - \lg k_{-1}|$. En comparant les valeurs du Tableau 1 à celles du Pt(II) de Kukushkin[7], nous obtenons:

$|\lg k_1 - \lg k_c| = 2{,}3$ (H_2O/NH_3), 3,3 (H_2O/en), 1,9 (H_2O/Me_4en) pour la substitution sur $PdCl_4^{2-}$ et respectivement 2,8, 3,5 et 1,9 pour $PtCl_4^{2-}$. De même:
$|\lg k_s - \lg k_{-1}| = 0{,}5$ (NH_3/Cl^-), 1,2 (en/Cl^-), 0,2 (Me_4en/Cl^-) pour la substitution sur $Pd(H_2O)Cl_3^-$ et > 2,4 (NH_3, en, Me_4en/Cl^-) pour $Pt(H_2O)Cl_3^-$.

Nous concluons que le pouvoir discriminatoire de $PtCl_4^{2-}$ est approximativement le même que celui de $PdCl_4^{2-}$. Par contre, l'aquocomplexe $Pt(H_2O)Cl_3^-$ discrimine davantage que celui du Pd(II). Dans ces rapports de réactivité, nous comparons toujours des substrats ayant la même charge, le même groupe *trans* et le même groupe de départ. Donc, dans le profil d'enthalpie libre de la réaction de substitution, la contribution de la formation de la liaison M—Y est relativement plus importante que la rupture de la liaison M—groupe de départ dans le cas de Pt(II) que dans celui de Pd(II).

Partie expérimentale

1. La technique cinétique et le traitement des données ont été décrits antérieurement[1]. Le détail des mesures et la préparation des complexes peuvent être obtenus à la Bibliothèque de l'Université de Lausanne[4].
2. Constantes de dissociation des diamines (chlorhydrates): $K_{a_1} = a_{H^+}[amH^+]/[amH_2^{2+}]$ et $K_{a_2} = a_{H^+}[am]/[amH^+]$ ont été déterminées par mesure potentiométrique du *p*H de solutions tampons[1] [25°, $[Cl^-] = 0{,}7$ M; $\mu = 1{,}0$ ($NaClO_4$)]; en: $pK_{a_1} = 7{,}53 \pm 0{,}01$, $pK_{a_2} = 10{,}23 \pm 0{,}01$; Me_2en: $7{,}56 \pm 0{,}01$, $10{,}18 \pm 0{,}04$; hp: $7{,}27 \pm 0{,}01$, $10{,}46 \pm 0{,}03$; Me_4en: $6{,}42 \pm 0{,}06$, $9{,}54 \pm 0{,}01$.

Nous remercions le Centre de calcul électronique de l'EPFL. Ce travail fait partie d'un projet (n° 2481.71) subventionné par le Fonds national suisse de la recherche scientifique, que nous remercions de son aide précieuse.

Bibliographie

1 R. Roulet et R. Ernst, *Helv. Chim. Acta 54* (1971) 2357.
2 L. I. Elding, *Inorg. Chim. Acta 6* (1972) 647.
3 R. A. Reinhardt et W. W. Monk, *Inorg. Chem. 9* (1970) 2026.
4 R. Ernst, Thèse, Faculté des Sciences de l'Université de Lausanne, 1973.
5 J. V. Rund, *Inorg. Chem. 9* (1970) 1211.
6 L. Cattalini, G. Marangoni, J. S. Coe, M. Vidali et M. Martelli, *J. Chem. Soc.* (A) *1971*, 593.
7 Y. N. Kukushkin et V. B. Ukraintsev, *Russ. J. Inorg. Chem. 15* (1970) 1269.
8 F. Basolo, H. B. Gray et R. G. Pearson, *J. Amer. Chem. Soc. 82* (1960) 4200.
9 L. I. Elding, *Inorg. Chim. Acta 6* (1972) 683.
10 L. I. Elding, *Acta Chem. Scand. 20* (1966) 2559.
11 F. Basolo et R. G. Pearson, *Mechanisms of inorganic reactions*, John Wiley, 1967.

R. Ernst et R. Roulet

Institut de chimie minérale et analytique,
Université de Lausanne
Place du Château 3, CH-1005 Lausanne

Metallorganische Azidokomplexe von Elementen der III. und IV. Hauptgruppe*

Summary

The complexes $Me_3SiN_3AlMe_3$ and $Me_3GeN_3GaMe_3$ are formed at low temperatures by reaction of the corresponding trimethylelementazides with the trimethylmetals of Al and Ga. At elevated temperatures the complexes decompose, whereby the species $[Me_2MN_3]_3$ were obtained. $[Me_2InN_3]_3$ was also prepared by an analogous route. The vibrational spectra of the trimeric azides with M = Ga, In were recorded and assigned.

Metallorganische Azidokomplexe des Typs $[R_3MN_3]^{\ominus}$ (I) sind befähigt, mittels des α-N-Atoms der N_3-Gruppe ein weiteres Akzeptormolekül MR_3 unter Bildung stabiler Komplexe $[R_3MN_3MR_3]^{\ominus}$ zu binden[1,2,3]:

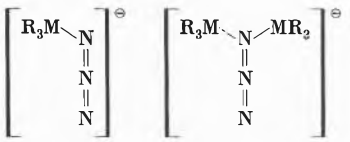

(I) (II)

M = Al, Ga
R = CH_3, C_2H_5

In diesem Zusammenhang interessierte uns die Frage, ob die zu (I) isoelektronischen Azide $(CH_3)_3SiN_3$ und $(CH_3)_3GeN_3$ mit Trimethylaluminium bzw. Trimethylgallium unter Bildung der zu (II) isoelektronischen Komplexe (IIIa bzw. IIIb) imstande sind, zumal Fluoride des Typs $R_3SiFAlR_3$ bis gegen 0 °C beständig sind[4]:

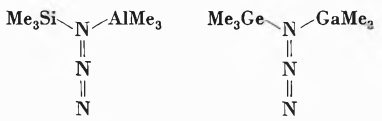

(IIIa) (IIIb)

Mit Hilfe der ^{1}H-Kernresonanzspektroskopie läßt sich zeigen, daß die Verbindungen (IIIa) und (IIIb) beim Mischen in dem für die Bildung der Komplexe notwendigen Mengenverhältnis der Komponenten $Me_3SiN_3/AlMe_3$ bzw. $Me_3GeN_3/GaMe_3$ innerhalb weniger Minuten bei − 10 °C bzw. − 32 °C gebildet werden. Die Ergebnisse der Messungen enthält Tabelle 1. Nach Homogenisierung der äquimolaren Mischung $Me_3SiN_3/\frac{1}{2}[AlMe_3]_2$ bei − 16 °C lassen sich zunächst (t_1) die CH-Singuletts der beiden Einzelkomponenten erkennen, die auch für das sowohl Brücken-CH_3- als auch terminale CH_3-Gruppen enthaltende $[(CH_3)_3Al]_2$ wegen des raschen CH_3-Austausches nur ein CH-Signal beobachten läßt.

Nach 20 Minuten (t_2) erhält man beim gleichzeitigen Anwärmen auf − 10 °C zwei neue Singuletts, von denen das der $Si(CH_3)_3$-Protonen nach tieferem Feld, das der $Al(CH_3)_3$-Protonen nach höherem Feld verschoben ist, was mit der durch die Komplexbildung (IIIa) veränderten Abschirmung der CH_3-Protonen im Einklang steht. Ähnliche Verhältnisse lassen sich im System $(CH_3)_3GeN_3/Ga(CH_3)_3$ feststellen, allerdings bei niedrigeren Temperaturen. Auffällig ist im Protonenspektrum des $[Me_3GeN_3GaMe_3]$-Komplexes die Hochfeldverschiebung auch der $Ge(CH_3)_3$-Protonen, die im Gegensatz zu der erwarteten Tieffeldverschiebung steht. Dies könnte ein Indiz für eine im flüssigen Zustand des $(CH_3)_3GeN_3$ bestehende intermolekulare Assoziation sein, wie sie mit Hilfe von ^{14}N-Kernresonanzspektren in der Reihe $Me_3SiN_3 - Me_3GeN_3 - Me_3SnN_3$ allerdings deutlich erst bei der Zinnverbindung in Erscheinung tritt[5].

Tabelle 1. ^{1}H-Kernresonanzspektren von Azidokomplexen. Chemische Verschiebungen in [τ], bezogen auf TMS extern

Zuordnung	$(CH_3)_3SiN_3Al(CH_3)_3$	$(CH_3)_3SiN_3$	$[Al(CH_3)_3]_2$	$(CH_3)_3SiN_3Al(CH_3)$
t_1 = 1 min [− 16 °C]	–	9,72	10,74	–
t_2 = 20 min [− 10 °C]	9,66	–	–	10,96
Zuordnung	$(CH_3)_3GeN_3Ga(CH_3)_3$	$(CH_3)_3GeN_3$	$Ga(CH_3)_3$	$(CH_3)_3GeN_3Ga(CH_3)_3$
t_1 = 1 min [− 36 °C]	9,87	9,36	10,18	10,18
t_2 = 10 min [− 32 °C]	9,87	–	–	10,22

* Eingegangen am 11. Juni 1974.

Tabelle 2. Auszüge aus den Massenspektren von $[(CH_3)_2MN_3]_3$ (M = Ga, In). Ionisierungsenergie 70 eV

$[(CH_3)_2GaN_3]_3$			$[(CH_3)_2InN_3]_3$		
m/e	Relative Häufigkeit [%]	Zuordnung	*m/e*	Relative Häufigkeit [%]	Zuordnung
414	~1	$^{71}Ga_3(CH_3)_5(N_3)_3^+$	545	~1	$^{115}In_3(CH_3)_5(N_3)_3^+$
412	~1	$^{69}Ga^{71}Ga_2(CH_3)_5(N_3)_3^+$	359	32,5	$^{115}In_2(CH_3)_3(N_3)_2^+$
410	~1	$^{69}Ga_2{}^{71}Ga(CH_3)_5(N_3)_3^+$	332	11,4	$^{115}In_2(CH_3)_4N_3^+$
408	~1	$^{69}Ga_3(CH_3)_5(N_3)_3^+$	302	3,3	$^{115}In_2(CH_3)_2N_3^+$
271	1,9	$^{71}Ga_2(CH_3)_3(N_3)_2^+$	274	4,9	$^{115}In_2(CH_3)_2N^+$
269	5,6	$^{69}Ga^{71}Ga(CH_3)_3(N_3)_2^+$	229	1,4	$^{115}In(CH_3)_2(N_3)_2^+$
267	3,5	$^{69}Ga_2(CH_3)_3(N_3)_2^+$	172	1,8	$^{115}In(CH_3)N_3^+$
143	~1	$^{71}Ga(CH_3)_2N_3^+$			
141	~1	$^{69}Ga(CH_3)_2N_3^+$			

Erwärmt man die Komplexe (IIIa) und (IIIb) einige Zeit auf Zimmertemperatur, so beobachtet man den Ablauf von Austauschreaktionen:

$$Me_3SiN_2AlMe_2 \rightarrow Me_4Si + Me_2AlN_3 \quad (1a)$$

$$Me_3GeN_3GaMe_3 \rightarrow Me_4Ge + Me_2GaN_3 \quad (1b)$$

Der Fortgang der Reaktionen (1a) und (1b) läßt sich kernresonanzspektroskopisch verfolgen. Nach beendeter Umsetzung lassen sich Me_2AlN_3 durch je ein Singulett bei τ = 10,58 und Me_2GaN_3 mit τ = 10,10 erkennen.

Die Verwendung von Trimethylsilylazid als Azidierungsmittel wurde zuerst von Wiberg et al.[6] beschrieben, die Me_3SiN_3 mit Me_2AlJ umsetzten und dabei $[Me_2AlN_3]_3$ erhielten, das mit dem nach Gl. (1a) erhaltenen und auch auf andere Weise[7] zugänglichen Präparat identisch ist. Wir fanden, daß außer Me_3GeN_3 [Gl. (1b)] auch Me_3SnN_3 und Me_3PbN_3 gegenüber den Trimethylverbindungen der Elemente der III. Hauptgruppe vorzügliche Azidierungsmittel sind, wobei in der Reihenfolge zunehmender Polarität der Metall–Azid-Bindung Me_3SiN_3, Me_3GeN_3, Me_3SnN_3, Me_3PbN_3 die Geschwindigkeiten der Austauschreaktionen vom Typ der Gleichung (1) sehr stark zunehmen. Wir nutzten diese Erfahrung zur Darstellung der bisher unbekannten Dimethylmetallazide von Gallium und Indium. Sie entstehen in praktisch vollständigen Ausbeuten z.B. nach (1b) bzw. (1c):

$$InMe_3 + Me_3SnN_3 \rightarrow Me_4Sn + Me_2InN_3 \quad (1c)$$

Beide Azide bilden ebenso wie die schon länger bekannten Diäthylazide von Al und Ga trimere Moleküle des Typs (IV):

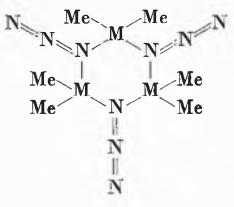

(IV)

Dafür sind die in Tabelle 2 enthaltenen Bruchstücke der Massenspektren, soweit sie für das vorliegende Problem interessieren, kennzeichnend.

Tabelle 3. Schwingungsspektren von $[(CH_3)_2MN_3]_3$ (M = Ga, In)

$[(CH_3)_2GaN_3]_3$				$[(CH_3)_2InN_3]_3$				Zuordnung
IR		Raman		IR		Raman		
cm^{-1}	Int.*	cm^{-1}	Int.	cm^{-1}	Int.	cm^{-1}	Int.	
				3390	s			
3337	s			3338	ss			$\nu_{as}N_3+\nu_sN_3$
2970	m	2970	ss	2980	s	2988	ss	
2920	s					2930	s	
		2903	m	2900	m	2910	s	νCH
				2850	ss			
				2720	ss			
2480	s			2650	ss			
				2310	ss			
2110	sst							
2105	Sch					2080	ss	$\nu'_{as}N_3$
2065	Sch			2060	sst	2042	s	
1440	s			1440	ss			$\delta_{as}CH_3$
				1369	ss			
1249	Sch	1245	st	1353	st	1348	st	ν_sN_3
1238	st			1295	m	1289	s	
1207	m-st	1210	m	1171	ss	1169	st	
1165	s			1166	ss	1163	m-st	δ_sCH_3
						1155	m	
				970	ss			
756	m-st			730	sst			ϱCH_3
720	st							$\varrho CH_3+\delta N_3$
700	Sch	700	ss			700	ss	ϱCH_3
602	m-st	598	m-st					$\nu_{as}GaC_2$
585	m			650	m			δN_3
				615	m			γN_3
				560	st	545	m	$\nu_{as}InC_2$
542	m	540	sst	493	s	488	sst	ν_sMC_2
415	m-st							νGa—N
369	m							νGa—N
				308	m			νM—N
270	m					260	s	
238	m-st	235	st					δMC_2
205	m-st							

* sst = sehr stark, st = stark, m = mittel, s = schwach, ss = sehr schwach, Sch = Schulter

Die Schwingungsspektren (Tabelle 3) lassen im Gegensatz zu den in flüssiger Phase planare Ringe (D_{3h}) bildenden Dialkylmetallaziden[7] $[(CH_3)_2AlN_3]_3$, $[(C_2H_5)_2AlN_3]_3$ und $[(C_2H_5)_2GaN_3]_3$ keine ebenen Ringe mehr zu. Informationen hierfür liefern u.a. das jeweils mehrfache Auftreten von asymmetrischer und

symmetrischer N_3-Valenzschwingung in beiden spektroskopischen Effekten (IR, Raman). Für die Abweichung von der Planarität der Ringe sind vermutlich die Packungsverhältnisse im kristallinen Zustand verantwortlich.

Die Raman-Spektren wurden mit Hilfe eines Laserstrahl-Geräts (5145 Å) des Typs Cary 83 registriert, die IR-Spektren wurden als Nujolverreibungen zwischen CsJ-Scheiben am Perkin-Elmer-Gerät 457 erhalten. Für die Massenspektren stand ein CH-4-Gerät der Atlas-Werke zur Verfügung, für die Kernresonanzspektren das Varian-Gerät XL 100.

Dem Fonds der Deutschen Chemischen Industrie danken wir für die großzügige Unterstützung.

Literatur

1 F. Weller und K. Dehnicke, *J. Organometal. Chem. 35* (1972) 237.
2 K. Dehnicke und I. L. Wilson, *J. Chem. Soc. Dalton 1973*, 1428.
3 J. L. Atwood und W. R. Newberry III., *J. Organometal. Chem. 65* (1974) 145.
4 H. Schmidbaur, *Fortschritte der Chemischen Forschung 13* (1969) 167.
5 J. Müller, *J. Organometal. Chem. 51* (1973) 119.
6 N. Wiberg, W. Ch. Joo und H. Henke, *Inorg. Nucl. Chem. Letters 3* (1967) 267.
7 J. Müller und K. Dehnicke, *J. Organometal. Chem. 12* (1968) 37.

N. Röder und K. Dehnicke

Fachbereich Chemie der Universität Marburg/Lahn
D-355 Marburg/Lahn, Lahnberge